Environmental Science & Technology

pubs.acs.org/est

Open Access

This article is licensed under CC-BY-NC-ND 4.0

Article

Process-Based and Probabilistic Quantification of Co and Ni Mobilization Risks Induced by Managed Aquifer Recharge

Claudio Vergara-Sáez, Henning Prommer,* Adam J. Siade, Jing Sun, and Simon Higginson

Cite This: *Environ. Sci. Technol.* 2024, 58, 7567−7576

Read Online

ACCESS | Metrics & More | Article Recommendations | Supporting Information

ABSTRACT: Managed aquifer recharge (MAR) is an increasingly used water management technique that enhances water availability while commonly generating water quality benefits. However, MAR activities may also trigger adverse geochemical reactions, especially during the injection of oxidant-enriched waters into reducing aquifers. Where this occurs, the environmental risks and the viability of mitigating them must be well understood. Here, we develop a rigorous approach for assessing and managing the risks from MAR-induced metal mobilization. First, we develop a process-based reactive transport model to identify and quantify the main hydrogeochemical drivers that control the release of metals and their mobility. We then apply a probabilistic framework to interrogate the inherent uncertainty associated with adjustable model parameters and consider this uncertainty (i) in long-term predictions of groundwater quality changes and (ii) in scenarios that investigate the effectiveness of modifications in the water treatment process to mitigate metal release and mobility. The results suggested that Co, Ni, Zn, and Mn were comobilized during pyrite oxidation and that metal mobility was controlled (i) by the sediment pH buffering capacity and (ii) by the sorption capacity of the native aquifer sediments. Both tested mitigation strategies were shown to be effective at reducing the risk of elevated metal concentrations.

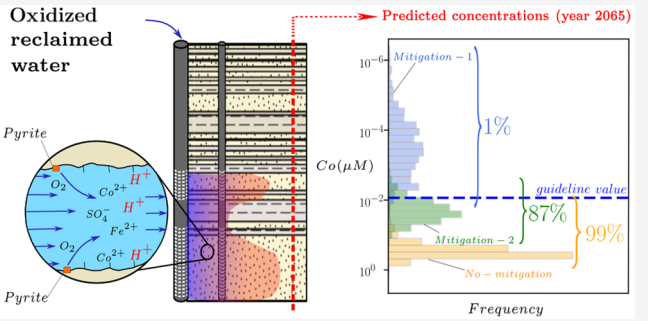

KEYWORDS: *managed aquifer recharge, metal mobility, reactive transport modeling, uncertainty, probabilistic framework*

Downloaded via CAOS NONCONSORTIA MBRS TRACKER on March 12, 2025 at 07:28:33 (UTC).
See https://pubs.acs.org/sharingguidelines for options on how to legitimately share published articles.

INTRODUCTION

Managed aquifer recharge (MAR), defined as the controlled replenishment of water into aquifers, is an increasingly used water management technique that enhances water availability while reducing both depletion of groundwater levels and evaporation losses.[1] MAR is often employed as a tool to mitigate the impacts of (i) naturally occurring seasonal variability, (ii) anthropogenic climate change impacts such as declining recharge rates, and (iii) rising water demands from population increase or industrial activities. However, while MAR schemes mostly generate beneficial effects on groundwater quality during MAR-induced subsurface passage and storage, there is also a risk of triggering undesirable geochemical reactions. Among the reported cases, where MAR created a groundwater quality deterioration (see, e.g., Fakhreddine et al.[2] for a recent review), the majority involved the mobilization of As.[3−9] Other geogenic contaminants have also been observed and the mechanistic processes underlying the MAR-induced mobilization have been examined for some of them, including F,[10] Mo,[11,12] Mn,[13,14] and Fe.[15] However, these studies generated single deterministic solutions while not paying attention to the effects of model uncertainty and its potential impact on predictions.

A range of different geochemical mechanisms can trigger the mobilization of metals and other contaminants. However, the oxidative dissolution of sulfide minerals, most commonly pyrite, has been identified as the leading cause for the repartitioning from solid-phase associations into groundwater, e.g., references[4,16−21]. In fact, as metal(oid)s such as As, Co, Ni, Mn, Zn, Mo, and Cd can substitute for Fe or S into the pyrite lattice,[22−27] they can be co-released during pyrite oxidation. For example, in the Surat Basin, Australia, the injection of co-produced water from coal seam gas operations has resulted in As mobilization.[6] In that case, the link between pyrite oxidation and As release was verified by a multistage push−pull experiment where the release of As occurred primarily when the injectant contained oxygen, while the injection of deoxygenated water largely inhibited pyrite oxidation, and thus, As release.[11]

Received: December 14, 2023
Revised: March 28, 2024
Accepted: March 28, 2024
Published: April 16, 2024

ACS Publications

© 2024 The Authors. Published by American Chemical Society

The release of protons during the oxidative dissolution of sulfides and the extent to which neutralization occurs has a crucial impact on the mobility of the released metal(loid)s transport, given that partitioning between aqueous and solid phase association is highly pH-dependent and metal(loid) mobility can change dramatically within a narrow pH range near each metals' sorption edge.[28−30] Where MAR activities induce metal mobilization, the larger-scale and longer-term environmental risks must be understood and adequately managed. Process-based reactive transport modeling provides a suitable framework for analyzing the fate of metals and predicting future groundwater quality evolution under natural and engineered conditions.[31,32] The development of such models relies on adequate groundwater quality monitoring data that can serve as constraints for the identification of conceptual models and numerical model parametrization. However, given the intrinsic complexity of the hydrogeological and geochemical processes controlling the fate of metals in heterogeneous subsurface environments, many model parameters cannot be uniquely estimated and remain uncertain. This uncertainty needs to be adequately propagated, where models are used for the determination of environmental risks.

In this study, we develop and apply a formal probabilistic uncertainty quantification for a reactive transport problem and demonstrate that such an approach leads to a more robust evaluation of contamination risks compared to a traditional deterministic approach. We illustrate an application of the approach for a case of MAR-induced metal mobilization. Our study consisted of three key steps: first, a single, highly likely model-based interpretation of field observations was performed to identify and quantify the most likely governing hydrogeochemical processes in the affected aquifer via history-matching. Second, the posterior parameter ensemble emerging from the parametric uncertainty of the model constructed in the previous step was employed in the predictions of the long-term behavior of the metals and for the quantification of the uncertainty of these predictions. Finally, two different mitigation options were evaluated comparatively with both the single model and the posterior ensemble. The effectiveness of the tested mitigations was then quantified, and the conclusions for decision-making from both approaches were compared in terms of their robustness.

MATERIAL AND METHODS

Study Site. In response to a drying climate and increasing water demands in Perth, Western Australia,[33] Groundwater Replenishment (GWR) has been developed as an additional domestic water supply source. GWR relies on the injection of highly treated recycled oxic water into the deep confined and anaerobic aquifer system that underlies the Perth Metropolitan area.[34] Prior to injection, the wastewater undergoes an advanced water treatment (AWT) process, which involves ultrafiltration (UF), reverse osmosis (RO), and UV disinfection, and leads to an injectant of very low ionic strength.[35] Following a closely monitored injection trial from 2010 to 2012,[35] the full-scale implementation of GWR in both the Leederville (∼125 to ∼225 m depth) and the Yarragadee aquifers (∼340 to ∼1,000 m depth) started in 2017, and is now one of the largest MAR operations for recycled water in the Southern Hemisphere.[34] During the entire injection trial and since the beginning of the full-scale GWR, groundwater quality monitoring results consistently complied with the applicable water quality guidelines, although a slight increase in fluoride and phosphate concentrations was observed.[10] Based on complementary lab experiments[10] and reactive transport modeling,[36] this increase was mechanistically linked to the dissolution of carbonate-rich fluorapatite and demonstrated to be a manageable groundwater quality risk.[37]

Recent monitoring results have, however, indicated rapidly increasing concentrations of Co, Ni, Zn, and Mn at a monitoring borehole, identified as Yarragadee Monitoring Bore 1 (YMB1), which serves as an early warning detection system for any undesired groundwater quality changes as it is located at a 50 m distance from the injection borehole Yarragadee Recharge Bore 1 (YRB1). Early detection of potential risks at this location allows for their mitigation prior to their propagation across the boundary of an area defined as a recharge management zone (RMZ), which was agreed upon among relevant stakeholders to be set at a radial distance of 250 m around the injection borehole. By December 2020, the highest measured concentrations at bore YMB1 were 0.17 μmol/L for Co, 0.34 μmol/L for Ni, 0.90 μmol/L for Zn, and 0.28 μmol/L for Mn. While the maximum Zn and Mn concentrations remained below the drinking water guideline values of 46.2 and 9.1 μmol/L, respectively,[38] Ni has reached the applicable guideline value of 0.34 μmol/L.[38] Furthermore, Co concentrations have already exceeded both the defined threshold that was agreed to by the various stakeholders of the GWR scheme (0.017 μmol/L)[39] and the health-based screening level based on non-cancer end points of 0.034 μmol/L.[40] The locations of YMB1, YRB1, and RMZ are provided in Figure S1.

Interestingly, the specific metals showing increased concentrations (i.e., Co, Ni, Zn, and Mn) closely correspond to those that were showing the highest concentration levels during earlier laboratory-scale incubation tests with sediment material from the upper Leederville aquifer.[30] In those tests, anaerobically collected aquifer material was exposed to constant oxygen levels while the geochemical response, including metal concentrations, was monitored in the aqueous phase.[30] Subsequent kinetic geochemical modeling of the experiments suggested that the observed metal release occurred in conjunction with the increasing levels of acidity that were created by the oxygen-induced pyrite oxidation and the relatively limited sediment buffering capacity.[30]

Overview of Modeling Tools and Procedures. Groundwater flow and reactive transport modeling, using MODFLOW[41] and PHT3D,[42] respectively, were used to examine and quantify the mechanisms involved in the MAR-induced release and fate of metals. Initial history matching was conducted via manual trial and error, followed by automated nonlinear regression using the Gauss−Levenberg−Marquardt (GLM) method coupled with Tikhonov regularization through the PESTPP-GLM code.[43] The parametric uncertainty of this single model was quantified by using an iterative ensemble smoother (IES), which is a state-of-the-art algorithm for history matching and uncertainty quantification regarding computationally expensive and high-dimensional applications. The IES is based on a Bayesian framework[44,45] and has been recently developed into a software tool.[43] Parameter sensitivities were quantified with the composite scaled sensitivity (CSS) indices, calculated through the PESTPP-GLM software tool.[43]

Model Framework and Boundary Conditions. Groundwater flow within the investigated aquifer section was assumed to be entirely driven by the injection of recycled water at bore

https://doi.org/10.1021/acs.est.3c10583
Environ. Sci. Technol. 2024, 58, 7567−7576

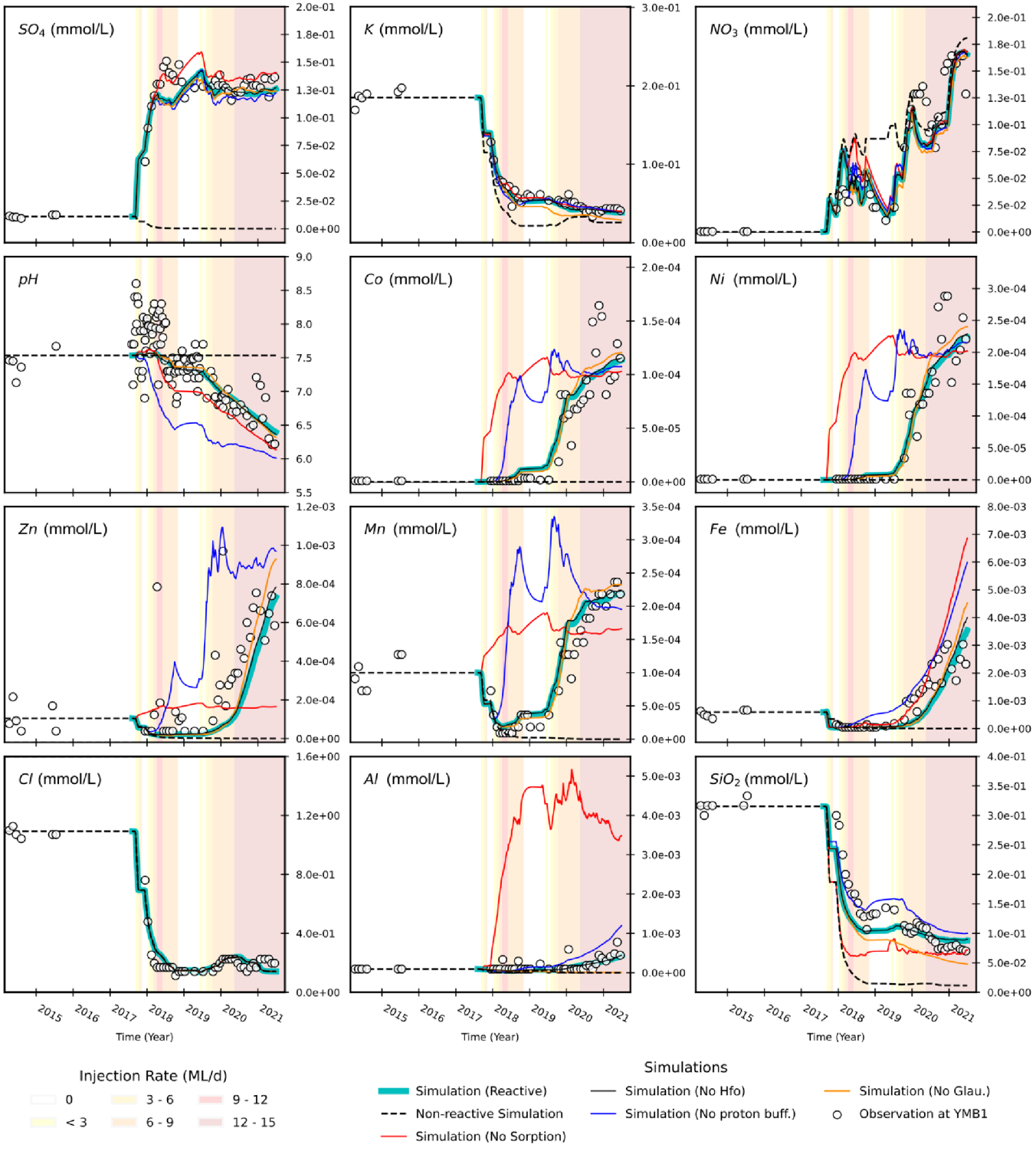

Figure 1. Observed and simulated breakthrough behavior of key species and pH variations at the monitoring bore YMB1. Cyan lines show the optimized reactive transport model using the estimated parameters from the GLM coupled with Tikhonov regularization, while black dashed lines show the non-reactive transport behavior. Comparative model simulations are shown for deactivated proton buffering reactions (blue lines); deactivated glauconite dissolution (orange lines); deactivation of the sorption capacity of any newly formed ferrihydrite (black straight lines); and deactivation of sorption capacity of the native Yarragadee sediments (red lines).

YRB1, while background groundwater flow was assumed to be negligible. Given this assumption, the model for the Yarragadee aquifer surrounding the injection well was set up as a radially symmetric flow and transport problem following the method proposed by Langevin[46] (Figure S2). Inflows were simulated by injection fluxes in the center of the radial model, while outflows were controlled by a constant head boundary located 1 km away from the injection bore. It was assumed that no vertical fluxes occurred across the model's top and bottom, and therefore, upper and lower boundaries were defined as

https://doi.org/10.1021/acs.est.3c10583
Environ. Sci. Technol. 2024, 58, 7567−7576

(natural) no-flow boundaries. The radially symmetric approach significantly reduces computational run times when assuming that lateral heterogeneity is negligible, as it is often valid in layered, subhorizontal formations, as observed at the study site.[47] The vertical domain was simulated as a single, vertically integrated layer using a dual-domain mass transfer (DDMT) model[48] to consider the impact of lithological heterogeneity on the reactive transport behavior in a computationally efficient manner. In the present case, sandy and therefore permeable aquifer sections are represented through the "mobile domain" fraction of the aquifer, whereas aquifer sections dominated by silts and clays were rather represented by the "immobile domain" fraction of the model domain. More details on the model development are provided in the Supporting Information. The conceptual hydrogeological model is illustrated in Figure S2.

Reaction Network. The reaction network that was used for the present study consists of a combination of equilibrium and kinetically controlled reactions that were defined in the PHREEQC/PHT3D reaction database.[42,49] Key aspects of the reaction network were already developed by earlier studies of the Perth deep aquifer system and demonstrated to capture many of the observed MAR-induced hydrogeochemical changes,[34,36,50,51] including the kinetically controlled redox processes (sulfide oxidation and SOM mineralization) as well as pH buffering processes (mineral and proton buffering, i.e., exchange of proton on cation exchanger sites).[32,51−55] In this study, additional modifications were implemented to account for (i) the release of the examined trace metals (Co, Ni, Mn, and Zn) and (ii) the surface complexation reactions that affect the mobility of these trace metals after mobilization. The full details of the implemented reaction network are provided in the Supporting Information.

Parameter Estimation and Predictive Uncertainty. Based on an initial qualitative sensitivity analysis, it was revealed that 26 parameters required formal estimation as these parameters seemed to exhibit significant controls on simulation results. This is an important step as the parameters considered during history-matching must, at a minimum, be those that control the salient processes in the underlying conceptual model that affect the model outcomes corresponding to observations. These parameters included selected reaction rate coefficients of kinetically controlled reactions, cation exchange capacity, surface site densities, background pyrite and glauconite concentrations, stoichiometric ratios of the trace metals within pyrite (Table S1), and equilibrium constants for the trace metal sorption reactions (Table S2). The measurements used for history-matching primarily corresponded to the concentrations of the elements closely linked to pyrite oxidation (Fe, SO_4, Co, Ni, Zn, Mn) and the groundwater pH. Additional concentrations of Na, Mg, Ca, K, F, PO_4, HCO_3, NH_4, Sr, Ba, Cl, NO_3, Si, and Al were also employed as constraints, although with lower weights.

Automated history-matching was performed in two steps: (i) employing the GLM algorithm and Tikhonov regularization to provide a single highly likely parameter estimate and (ii) applying the iterative ensemble smoother (IES) to provide an estimate of parameter uncertainty based on an ∼800-member ensemble of history-matched model realizations. The ∼800-member posterior parameter ensemble was subsequently used to quantify predictive uncertainty, a primary objective of this study, by executing them through an extension of the model to simulate metal concentrations at the RMZ boundary for a predictive period of ∼50 years beyond 2021. Assuming that parameter uncertainty is the main source of predictive uncertainty, the estimated distributions of metal concentrations were considered to be a representative sample of the future probability distribution. Accordingly, a risk analysis was conducted based on the probability that the predicted concentrations would exceed their defined guideline values. The probabilistic results and the single results from the Tikhonov regularized model were compared in terms of their robustness for decision-making. Additional details on the automated history-matching are provided in Section 2.3 of the Supporting Information.

Parameter Sensitivities and Identifiabilities. Parameter sensitivities were derived via linearization, i.e., by calculating the so-called composite scaled sensitivities,[43] which represent the linearized influence of individual parameters on model outputs. Parameter identifiabilities[56−58] were estimated by calculating the reduction of the posterior parameter standard deviations (SD) from the prior parameter SD.

Mitigation Scenarios. Potential strategies to reduce metal release and/or mobility were investigated based on the identified GWR-induced geochemical processes and the level of risk revealed by the uncertainty analysis. Two key scenarios, which correspond to two readily implementable mitigation options, were simulated: (i) deoxygenation of the injected water, as it has previously demonstrated to prevent metal(loid) mobilization,[11,59] and (ii) increase of bicarbonate concentration in the injected water to improve the intrinsic buffering capacity of the injectant, as previously proposed by Sun et al.[34] Finally, the effectiveness of these mitigation scenarios was assessed by comparing the percentage of model realizations (from the ∼800-member ensemble) that predicted concentrations above the guideline value for the entire prediction period. Additional comparisons were made for the predicted probability distributions of the concentrations in 2065.

RESULTS AND DISCUSSION

Hydrogeochemical Evolution at the Early Warning Monitoring Bore YMB1. The majority of the observed hydrogeochemical changes at YMB1 were found to be dominated by (i) the displacement of the anoxic ambient groundwater by the low-ionic-strength, oxidized injectant and (ii) the reactions between the oxidized injectant and the reducing aquifer. The conservative transport behavior that resulted from the induced radial flow field is most clearly illustrated by the simulated (and observed) concentrations of chloride, which show a sudden decrease in concentrations at ∼8 months after the start of the injection in Aug 2017 (Figure 1). On the other hand, the key reactive processes between the oxidized injectant and the reducing background groundwater were found to be (i) pyrite oxidation by dissolved oxygen and nitrate, as the primary driver of redox changes and the associated release of acidity, (ii) proton exchange, as the main pH buffering reaction in response to the acidification, and (iii) sorption capacity of the native sediments, primarily controlled by the pH. Matching the observed behavior with the model simulations was shown to be a crucial prerequisite for accurately describing the reactive processes, as pyrite oxidation, sorption processes, and buffering reactions control the long-term evolution of the groundwater pH and the metal breakthrough.

The occurrence of pyrite oxidation is mostly evidenced from the simulated groundwater sulfate concentrations that agree

https://doi.org/10.1021/acs.est.3c10583
Environ. Sci. Technol. 2024, 58, 7567−7576

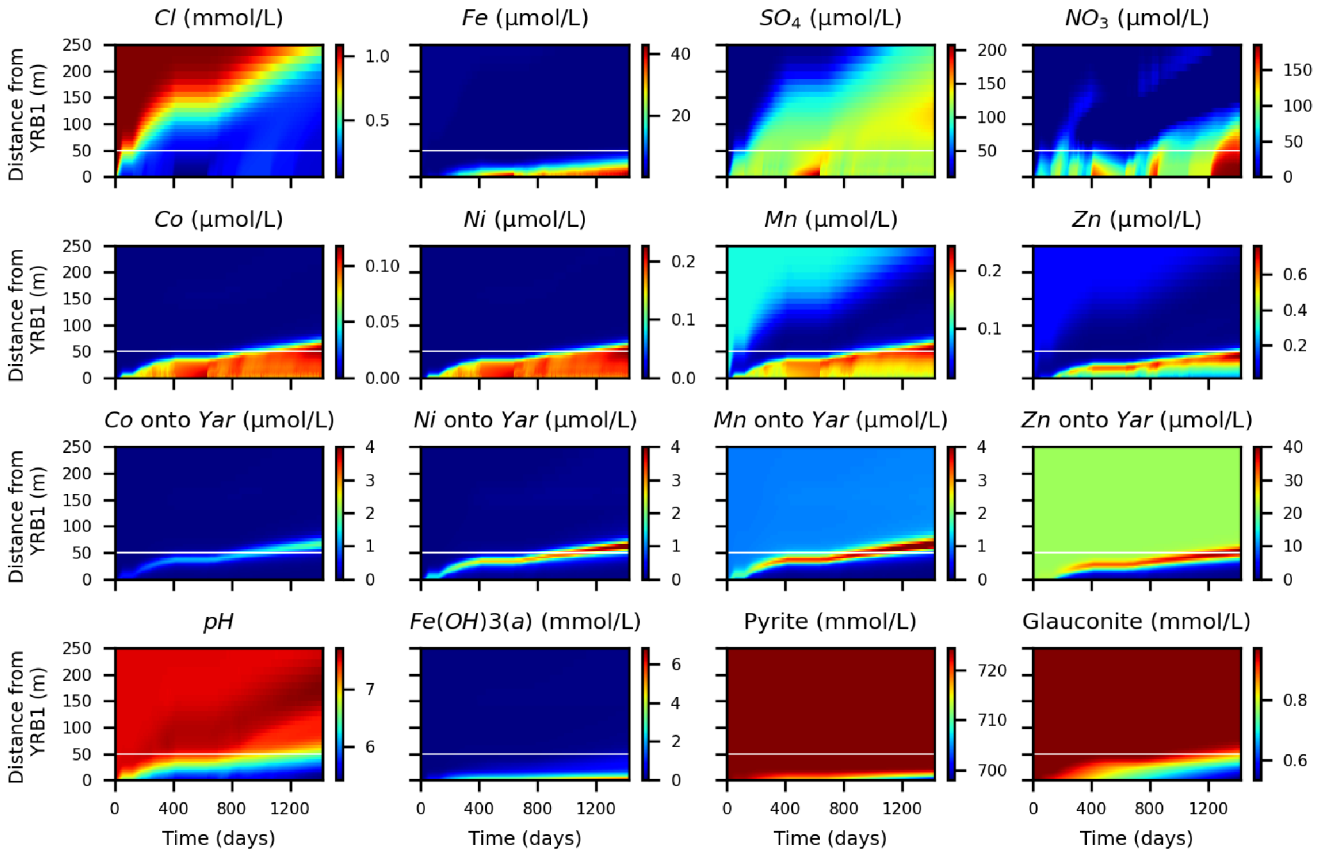

Figure 2. Spatiotemporal variations of MAR-induced hydrogeochemical changes. The vertical axis displays the model extent in radial direction between the injection bore YMR1 (bottom) and the RMZ boundary (top). The horizontal white lines indicate the location of monitoring bore YMB1. The horizontal axis indicates the temporal changes, clearly illustrating the migration of the acidification front. "Metal onto Yar" represents metal sorption onto the native sediments in the Yarragadee aquifer. Note that elevated dissolved metal concentrations are mostly found within the low-pH zone. Metal accumulation sorption occurs just beyond the pH transition zone, where pH has remained circumneutral.

only with observed concentrations when pyrite oxidation was included in the reaction network. This behavior is consistent with previous observations and simulations of MAR-induced geochemical changes in the Leederville aquifer in Perth's deep aquifer system,[34,35,51] Furthermore, the observed successively declining pH at YMB1 was matched well by including proton exchange as the main pH buffering process.[34,51] When proton exchange was not considered (blue lines in Figure 1), the simulated pH at YMB1 underestimated the observed pH by almost 0.8 units. This model variant shows that pH rapidly decreased from 7.5 to 6.4 just before the injection was interrupted in Oct 2018, while, in comparison, the observations still showed a relatively constant pH. Conversely, glauconite dissolution was also tested as a potential pH buffering process; however, the model variant without glauconite shows no changes in either the simulated pH trend or the breakthrough behavior of any of the cations that glauconite bears.

A closer inspection of the simulation results shows that the acidification front generated by pyrite oxidation remains confined to the vicinity of the injection bore (~37 m in radial distance) at the end of the history-matching period, i.e., June 2021 (Figure 2). At this location, the simulated pH decreases to 4.8. Between 37 and 65 m from YRB1, the groundwater pH shows a gradual transition to circumneutral values, while further away, the groundwater remains at the background value of ~7.5. Overall, the reactive transport model simulations were able to closely reproduce the breakthrough behavior of most measured cations and anions during the entire model calibration period (Figure 1). Additional breakthrough curves are provided in Figure S3.

MAR-Induced Trace Metal Release and Attenuation. The breakthrough behavior of the trace metals that was observed at YMB1 was also well reproduced by the reactive transport simulations (cyan lines in Figure 1). This favorable agreement supports the hypothesis that pyrite oxidation is the key control for the release of the trace metals, while the temporally and spatially varying extent of surface complexation reactions controls the migration rates of the metals in the groundwater after their release. The model-estimated stoichiometric ratios of trace metals in pyrite, which controls the magnitude of metal release, are summarized in Table S1.

The importance of the aquifer's buffering capacity on metal mobility is illustrated by the comparative model simulation in which proton exchange, as the main driver for pH buffering, is deactivated. In that case, dissolved Co, Ni, Mn, and Zn increase rapidly and much earlier than observed even when sorption reactions are considered. Additional comparative model simulations were conducted by deactivating the different sorption reactions (onto the native sediments and onto newly formed ferrihydrite) to examine their relative importance in controlling metal mobility. The results showed that metal sorption is dominated by native aquifer sediments. This is most clearly observed when deactivating the sorption

https://doi.org/10.1021/acs.est.3c10583
Environ. Sci. Technol. 2024, 58, 7567−7576

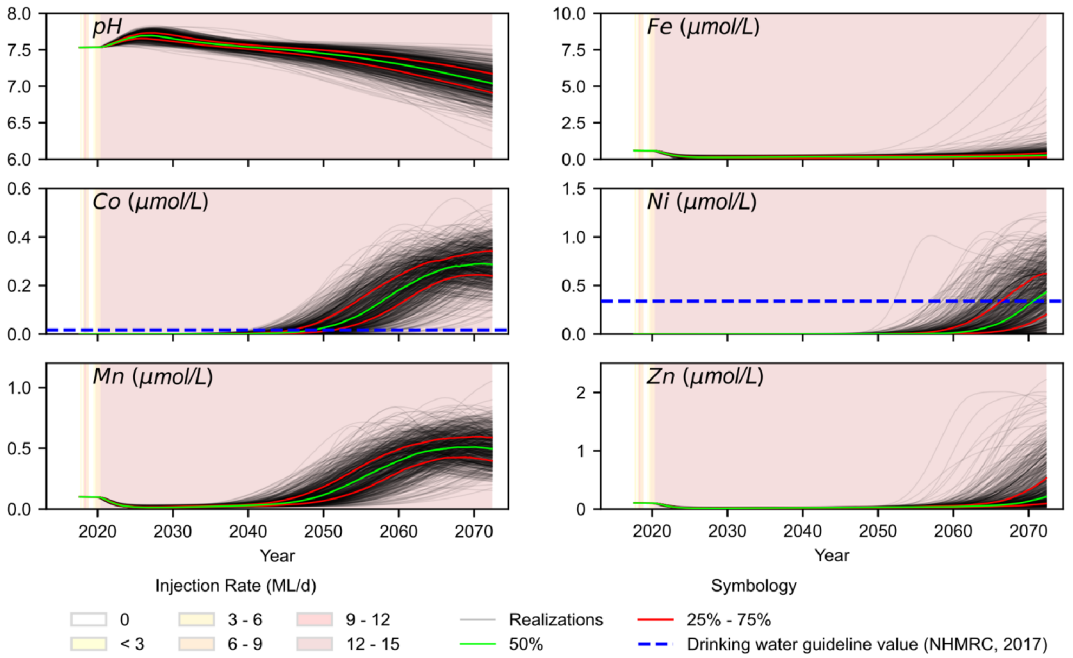

Figure 3. Predicted concentration at the RMZ boundary for ∼50 years after June 2021 assuming a constant injection rate of 10 ML/day. Gray lines show individual realizations of the ∼800-member ensemble. Green lines represent the median concentration, while red lines show the first and third quartiles. Dashed blue horizontal lines show drinking water guideline values for Ni (0.34 μmol/L; 0.02 mg/L) and Co (0.017 μmol/L; 0.001 mg/L) defined by NHMRC[38] and Water Corporation,[39] respectively. Note that first arrival of elevated concentration of Co and Ni are predicted to occur ∼31 years (∼year 2048) and ∼50 years (∼year 2070) since the start of the injection in 2017. Other key species, including Zn, Mn, Fe, and Al, are not expected to occur at elevated concentration at the RMZ boundary during the next 50 years.

on the native sediments (red lines in Figure 1). In this simulation, the breakthrough of Co, Ni, Mn, and Zn occurs almost immediately after the beginning of the injection. In contrast, sorption to neo-precipitated ferrihydrite had a negligible impact, as demonstrated by the simulations in which metal sorption onto ferrihydrite was excluded (black straight lines in Figure 1). This point is also illustrated in Figure 2, which shows that ferrihydrite precipitation was mostly limited to the immediate vicinity of the injection well, and therefore, the newly created sorption capacity remained restricted.

This influence of the sorption capacity of the Yarragadee sediments on Co, Ni, Mn, and Zn mobility is best observed when examining how the front of elevated metal concentrations is confined to the zone where most metals are being sorbed (Figure 2). Moreover, Figure 2 illustrates that this zone of maximum metal sorption is located just beyond the front of the low-pH zone, where mobilized metals can be attenuated by sorption reactions and accumulate under circumneutral pH conditions. In turn, maximum dissolved metal concentrations are found within the zone occupied by the more acidic groundwater. Accordingly, the sorption capacity of the Yarragadee sediments represents the main control on the mobility of metals, which in turn is controlled by the groundwater pH.

Parameter Sensitivities, Posterior Parameter Distributions, and Uncertainty Quantification. The most identifiable parameters of the model were found to be (i) the surface site density of the native sediments, (ii) the exchanger density of the exchanger Y sites, (iii) the initial pyrite concentrations, and (iv) the exchanger density of the exchanger X sites (Table S1, Figures S4 and S5). Additionally, these parameters show comparatively large CSS indices, supporting the hypothesis that the main hydrogeochemical controls in the release and migration of the metals are indeed pyrite oxidation, sorption processes, and buffering reactions. On the other hand, the least identifiable parameters were (i) immobile porosity, (ii) most of the equilibrium constant for sorption reactions (except that of Mn), (iii) Fe^{2+} oxidation rates, (iv) the surface site density of the newly formed ferrihydrite, (v) the term for oxygen-driven SOM degradation, and (vi) the stoichiometric ratio of Zn in pyrite (Table S1, Figures S4 and S5). It is interesting to note that while the stoichiometric ratio of Zn showed a small SD reduction, its sensitivity was calculated as one of the largest among the estimated parameters. This implies that even though this parameter is sensitive to the model, it is likely to be highly correlated to other parameters, in this case, Co, Ni, and Mn stoichiometric ratios.

It is important to note that this analysis assumes that prior PDFs are well defined for all of the parameters. However, the parameter ranges for the equilibrium constants describing the sorption reactions, as defined by upper and lower bounds, were directly adopted from the literature values for sorption onto ferrihydrite.[60] This was done in the absence of site-specific sorption experiments, even though sorption site hosts were not dominated by ferrihydrite. As a result, the identifiability and global sensitivity of these parameters may have been underestimated due to the restricted or potentially shifted ranges of the defined prior PDFs. For example, the posterior PDF of the equilibrium constant of the sorption of Mn onto the weak sites of the native sediment appears to be shifted to lower values, which may indicate that the real log K values are outside the provided range for ferrihydrite.[60] Histograms of the prior and posterior distributions of all model parameters are provided in Figure S4.

https://doi.org/10.1021/acs.est.3c10583
Environ. Sci. Technol. 2024, 58, 7567−7576

Predicted Long-Term Trace Metal Behavior. Arrival times were estimated using the 50% quartile curves, i.e., the curves defined by the median values of the Co, Ni, Mn, and Zn predicted concentrations from the ∼800 model realizations (green lines in Figure 3). Accordingly, the arrival times of Mn, Co, Ni, and Zn at the RMZ boundary were predicted to occur in ∼2040, ∼ 2045, ∼ 2057, and ∼2062, respectively. The difference in the arrival times is largely the result of the spatially and temporally varying pH conditions (Figure 2) that control the metal sorption onto the Yarragadee native sediments. The results correspond closely with the sorption affinity of these metals to ferrihydrite.[28,60,61] Predicted concentrations of additional species are shown in Figure S6.

Co concentrations exceeding the guideline value of 0.017 μmol/L[39] are predicted to arrive at the RMZ boundary in ∼2048 (based on the 50% quartile curves as an indicator of a preeminent risk), while concentrations of Ni above its guideline value of 0.34 μmol/L[38] are expected to occur from ∼2070 onward (Figure 3). No other metals were found to exceed their respective guideline values at or beyond the RMZ boundary, including Zn, Mn, and Fe. The ∼800-member ensemble showed that ∼100% of the realizations presented concentrations above the guideline value for Co by 2065 (Figure 4). This implies that, without the implementation of

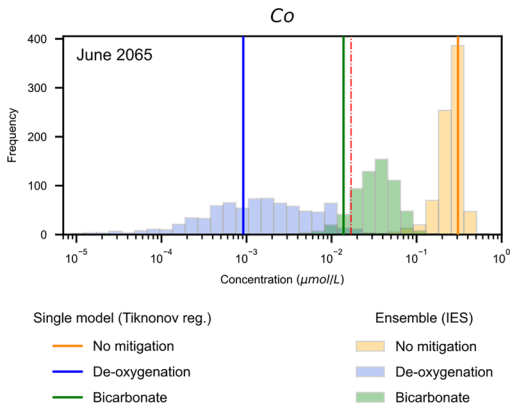

Figure 4. Comparison of the probability distribution of simulated concentrations at the RMZ boundary as a measure of the effectiveness of the tested mitigation strategies. Without mitigation, ∼100% of the realizations showed a guideline exceedance for the concentrations of Co at the RMZ boundary after ∼2065. Deoxygenation achieved near 100% mitigation effectiveness, while raising the alkalinity of the injectant showed around 87% of the realizations an exceedance of Co concentrations above the guideline value (dashed red line).[39] Note that results obtained from the single-run outputs from the Tikhonov regularization show Co concentrations lower than the guideline value after both mitigation were tested, which is not likely to be the case for the bicarbonate mitigation strategy. This could lead to biased decisions when not considering a more robust probabilistic approach.

suitable mitigation strategies, Co concentrations could exceed guideline values from 2048 onward (Figure 3). On the other hand, 21% of the realizations showed that Ni will exceed its guideline value by 2065 (Figure S7). Although a fifth of the realizations exceed the guideline values, the risk of elevated concentrations of Ni arriving at the RMZ boundary is very low in comparison to the exceedance risk for Co.

Effectiveness of Mitigation Options. Based on the predicted risk for guideline exceedances at and beyond the RMZ boundary, possible mitigation strategies were tested through predictive simulations. The results show that while some realizations predicted concentrations of Co above the guideline value after deoxygenating the injected water, the probabilistic results demonstrate that the risk of guideline exceedance was found to be near 0% for the entire simulation period (Figures 4 and S9). Similar results were found for predicted Ni concentrations (Figures S7 and S9). On the other hand, the effectiveness of raising bicarbonate levels in the injectant was found to be less effective than deoxygenation. In this case, around 87% of the realizations were found to exceed the guideline value of Co by 2065 (Figures 4 and S8), while no realization exceeded the guideline value of Ni by 2065 (Figures S7 and S8). Nonetheless, other aspects that may need to be considered in decision-making are that deoxygenation has the benefit of inhibiting the release of both positively and negatively charged contaminants, while raising the alkalinity and pH bears the risk of increasing the mobility of, for example, As. On the other hand, deoxygenation is rather cost- and energy-intensive, and would only be applied where raising the alkalinity is at risk of failing mitigation targets.

If decisions were to be made using the single Tikhonov parameter set, there would be significant potential for failure in meeting management objectives. In fact, decision-makers could be tempted to raise alkalinity based solely on these results, as this is a more economical alternative to deoxygenation and its predicted concentrations of Co were found to be lower than the guideline value (Figure 4). However, applying this strategy can lead to a high risk of exceeding Co guidelines by 2065 as concluded from the probabilistic results (Figure 4). These findings support our hypothesis that a formal probabilistic quantification of uncertainty is a more robust methodology for risk assessment than the common practice of using a single "calibrated" (deterministic) model to underpin management decisions.

Environmental Implications. This study developed a process-based framework to evaluate the MAR-induced metal mobilization risks based on hydrogeochemical data collected before and after the start of large-scale groundwater replenishment of Perth's deep aquifer system. The first step involved the development, evaluation, and refinement of a conceptual hydrogeochemical model of the controlling geochemical processes and its numerical implementation. The numerical model development resulted in a highly parametrized model for which the parameter uncertainty was quantified prior to employing the simulation model for predicting long-term groundwater quality impacts to assess predictive uncertainty. For our study site, the history-matching process and additional comparative model simulations clearly illustrate that pyrite oxidation was the main driver to facilitate metal release, while metal migration rates are mostly controlled by the progression of an acidification front that successively intrudes further into the aquifer sections surrounding the injection bore location. The rate at which the acidification progresses closely correlates with the rate at which the sediment's pH buffering capacity becomes depleted. Conceptually, the observed behavior and its controls correspond closely to those found at many acid mine drainage (AMD) sites around the world.[62−64] However, due to the limited oxidation capacity contained in the injectant, the release of acidity remains far less extreme compared to typical AMD cases and shows, in our study, amenability to mitigation through relatively simple changes in the AWT process.

The developed modeling framework illustrates the advantages of a highly parametrized, process-based, quantitative approach in selecting and designing mitigation strategies that

https://doi.org/10.1021/acs.est.3c10583
Environ. Sci. Technol. 2024, 58, 7567−7576

reduce groundwater contamination risks under uncertainty. Given the substantial infrastructure and operating costs of MAR schemes that rely on AWT processes, numerical modeling provides a necessary tool to safeguard groundwater quality in aquifers targeted by MAR schemes. Although our tested mitigation strategies are site-specific, they have been broadly applied to AMD-affected sites and many other MAR sites. In fact, it has been previously demonstrated that regardless of pH, deoxygenation greatly reduces the mobilization of As.[2,6,11,65] However, the results of these previous studies were based on a single model or using several history-matched-constrained models with a small number of parameters to reduce computational requirements.[6] Conversely, as our probabilistic approach relies on a computationally effective Bayesian framework, it can serve as a template for other MAR sites that are at risk from metal mobilization or other types of groundwater quality deterioration, including those with negatively charged contaminants, regardless of the complexity of their governing hydrogeochemical processes. It is important to note that in the present study, predictive uncertainty emerged solely from model parameter uncertainty, while conceptual model uncertainty was not excessively investigated. This approach is most likely justified by the rich history of a combined comprehensive observation data collection paired with a continuous interrogation of the collected data through flow, solute, and reactive transport modeling studies. These have provided a relatively firm conceptual understanding of the key physical and geochemical processes, which may not be available for other sites, thus potentially requiring consideration of conceptual uncertainties in any forward predictions.

■ ASSOCIATED CONTENT

Supporting Information

The Supporting Information is available free of charge at https://pubs.acs.org/doi/10.1021/acs.est.3c10583.

Estimated model parameter (Table S1); estimated equilibrium constants for sorption reactions (Table S2); surface complexation database (Table S3); study site location (Figure S1); model setup (Figure S2); additional breakthrough curves of species included in the calibration process (Figure S3); prior and posterior distribution of parameters (Figure S4); parameter identifiabilities and sensitivities (Figure S5); predicted concentrations of additional species (Figure S6); probability distribution of Co and Ni concentrations at the RMZ in 2055 and 2065 (Figure S7); and predicted concentrations after mitigation options are applied (Figures S8 and S9) (PDF)

■ AUTHOR INFORMATION

Corresponding Author

Henning Prommer − *School of Earth Sciences, University of Western Australia, Perth, Western Australia 6009, Australia; CSIRO Environment, Wembley, Western Australia 6913, Australia;* orcid.org/0000-0002-8669-8184; Phone: +61 8 93336272; Email: Henning.Prommer@uwa.edu.au; Fax: +61 8 9333 6499

Authors

Claudio Vergara-Sáez − *School of Earth Sciences, University of Western Australia, Perth, Western Australia 6009, Australia; CSIRO Environment, Wembley, Western Australia 6913, Australia*

Adam J. Siade − *School of Earth Sciences, University of Western Australia, Perth, Western Australia 6009, Australia; CSIRO Environment, Wembley, Western Australia 6913, Australia;* orcid.org/0000-0003-3840-5874

Jing Sun − *School of Earth Sciences, University of Western Australia, Perth, Western Australia 6009, Australia; CSIRO Environment, Wembley, Western Australia 6913, Australia; State Key Laboratory of Environmental Geochemistry, Institute of Geochemistry, Chinese Academy of Sciences, Guiyang 550081, China;* orcid.org/0000-0002-0129-5184

Simon Higginson − *Water Corporation of Western Australia, Leederville, Western Australia 6007, Australia*

Complete contact information is available at: https://pubs.acs.org/10.1021/acs.est.3c10583

Notes

The authors declare no competing financial interest.

■ ACKNOWLEDGMENTS

This study was supported by the Water Corporation of Western Australia, the Commonwealth Scientific and Industry Research Organization (CSIRO), the National Research and Development Agency of the Republic of Chile (ANID), the Richard G. Barnes bursary of hydrogeology from the University of Western Australia, and the Forrest Research Foundation. History-matching, uncertainty analysis, and parameter sensitivity were performed using 1000 cores on CSIRO's 230-node Dell high-performance computer (HPC) cluster "Petrichor".

■ REFERENCES

(1) Dillon, P.; Stuyfzand, P.; Grischek, T.; Lluria, M.; Pyne, R. D. G.; Jain, R. C.; Bear, J.; Schwarz, J.; Wang, W.; Fernandez, E.; et al.et al Sixty years of global progress in managed aquifer recharge. *Hydrogeol. J.* **2019**, *27* (1), 1−30.

(2) Fakhreddine, S.; Prommer, H.; Scanlon, B. R.; Ying, S. C.; Nicot, J.-P. Mobilization of Arsenic and Other Naturally Occurring Contaminants during Managed Aquifer Recharge: A Critical Review. *Environ. Sci. Technol.* **2021**, *55* (4), 2208−2223.

(3) Wallis, I.; Prommer, H.; Simmons, C. T.; Post, V.; Stuyfzand, P. J. Evaluation of Conceptual and Numerical Models for Arsenic Mobilization and Attenuation during Managed Aquifer Recharge. *Environ. Sci. Technol.* **2010**, *44* (13), 5035−5041.

(4) Wallis, I.; Prommer, H.; Pichler, T.; Post, V.; Norton, S. B.; Annable, M. D.; Simmons, C. T. Process-Based Reactive Transport Model To Quantify Arsenic Mobility during Aquifer Storage and Recovery of Potable Water. *Environ. Sci. Technol.* **2011**, *45* (16), 6924−6931.

(5) Vanderzalm, J. L.; Dillon, P. J.; Barry, K. E.; Miotlinski, K.; Kirby, J. K. Arsenic mobility and impact on recovered water quality during aquifer storage and recovery using reclaimed water in a carbonate aquifer. *Appl. Geochem.* **2011**, *26* (12), 1946−1955.

(6) Rathi, B.; Siade, A. J.; Donn, M. J.; Helm, L.; Morris, R.; Davis, J. A.; Berg, M.; Prommer, H. Multiscale Characterization and Quantification of Arsenic Mobilization and Attenuation During Injection of Treated Coal Seam Gas Coproduced Water into Deep Aquifers. *Water Resour. Res.* **2017**, *53* (12), 10779−10801.

(7) Vanderzalm, J. L.; Page, D. W.; Barry, K. E.; Scheiderich, K.; Gonzalez, D.; Dillon, P. J. Probabilistic Approach to Evaluation of Metal(loid) Fate During Stormwater Aquifer Storage and Recovery. *Clean: Soil, Air, Water* **2016**, *44* (12), 1672−1684.

(8) Fakhreddine, S.; Prommer, H.; Gorelick, S. M.; Dadakis, J.; Fendorf, S. Controlling Arsenic Mobilization during Managed Aquifer Recharge: The Role of Sediment Heterogeneity. *Environ. Sci. Technol.* **2020**, *54* (14), 8728−8738.
(9) Stuyfzand, P. J. Quality changes upon injection into anoxic aquifers in the Netherlands: Evaluation of 11 experiments. In *Proceedings of the 3rd International Symposium on the Artificial Recharge of Ground Water, Amsterdam*; Peters, J., Ed.; Balkema, 1998; pp. 283291.
(10) Schafer, D.; Donn, M.; Atteia, O.; Sun, J.; MacRae, C.; Raven, M.; Pejcic, B.; Prommer, H. Fluoride and phosphate release from carbonate-rich fluorapatite during managed aquifer recharge. *J. Hydrol.* **2018**, *562*, 809−820.
(11) Prommer, H.; Sun, J.; Helm, L.; Rathi, B.; Siade, A. J.; Morris, R. Deoxygenation Prevents Arsenic Mobilization during Deepwell Injection into Sulfide-Bearing Aquifers. *Environ. Sci. Technol.* **2018**, *52* (23), 13801−13810.
(12) Koopmann, S.; Prommer, H.; Siade, A.; Pichler, T. Molybdenum Mobility During Managed Aquifer Recharge in Carbonate Aquifers. *Environ. Sci. Technol.* **2023**, *57*, 7478.
(13) Oren, O.; Gavrieli, I.; Burg, A.; Guttman, J.; Lazar, B. Manganese Mobilization and Enrichment during Soil Aquifer Treatment (SAT) of Effluents, the Dan Region Sewage Reclamation Project (Shafdan), Israel. *Environ. Sci. Technol.* **2007**, *41* (3), 766−772.
(14) Zuurbier, K. G.; Hartog, N.; Stuyfzand, P. J. Reactive transport impacts on recovered freshwater quality during multiple partially penetrating wells (MPPW-)ASR in a brackish heterogeneous aquifer. *Appl. Geochem.* **2016**, *71*, 35−47.
(15) Lee, W.; Bresciani, E.; An, S.; Wallis, I.; Post, V.; Lee, S.; Kang, P. K. Spatiotemporal evolution of iron and sulfate concentrations during riverbank filtration: Field observations and reactive transport modeling. *J. Contam. Hydrol.* **2020**, *234*, 103697.
(16) Battistel, M.; Stolze, L.; Muniruzzaman, M.; Rolle, M. Arsenic release and transport during oxidative dissolution of spatially-distributed sulfide minerals. *J. Hazard. Mater.* **2021**, *409*, 124651.
(17) Candeias, C.; Ávila, P. F.; Da Silva, E. F.; Ferreira, A.; Durães, N.; Teixeira, J. P. Water−Rock Interaction and Geochemical Processes in Surface Waters Influenced by Tailings Impoundments: Impact and Threats to the Ecosystems and Human Health in Rural Communities (Panasqueira Mine, Central Portugal). *Water, Air, Soil Pollut.* **2015**, *226* (2), 1−30.
(18) Neil, C. W. Understanding the Nano- and Macroscale Processes Impacting Arsenic Mobilization during Managed Aquifer Recharge using Reclaimed Wastewater. Theses & Dissertations, 2015.
(19) Antoniou, A.; Stuyfzand, P.; van Breukelen, B. Reactive transport modeling of an aquifer storage and recovery (ASR) pilot to assess long-term water quality improvements and potential solutions. *Appl. Geochem.* **2013**, *35*, 173−186.
(20) Vandenbohede, A.; Wallis, I.; Alleman, T. Trace metal behavior during in-situ iron removal tests in Leuven, Belgium. *Sci. Total Environ.* **2019**, *648*, 367−376.
(21) Larsen, F.; Postma, D. Nickel Mobilization in a Groundwater Well Field: Release by Pyrite Oxidation and Desorption from Manganese Oxides. *Environ. Sci. Technol.* **1997**, *31* (9), 2589−2595.
(22) Price, R. E.; Pichler, T. Abundance and mineralogical association of arsenic in the Suwannee Limestone (Florida): Implications for arsenic release during water-rock interaction. *Chem. Geol.* **2006**, *228*, 44−56.
(23) Steadman, J. A.; Large, R. R.; Olin, P. H.; Danyushevsky, L. V.; Meffre, S.; Huston, D.; Fabris, A.; Lisitsin, V.; Wells, T. Pyrite trace element behavior in magmatic-hydrothermal environments: An LA-ICPMS imaging study. *Ore Geol. Rev.* **2021**, *128*, 103878.
(24) Jones, G. W.; Pichler, T. Relationship between Pyrite Stability and Arsenic Mobility During Aquifer Storage and Recovery in Southwest Central Florida. *Environ. Sci. Technol.* **2007**, *41* (3), 723−730.
(25) Houben, G. J.; Sitnikova, M. A.; Post, V. E. A. Terrestrial sedimentary pyrites as a potential source of trace metal release to groundwater − A case study from the Emsland, Germany. *Appl. Geochem.* **2017**, *76*, 99−111.
(26) Roberts, F. I. Trace element chemistry of pyrite: A useful guide to the occurrence of sulfide base metal mineralization. *J. Geochem. Explor.* **1982**, *17* (1), 49−62.
(27) Abraitis, P. K.; Pattrick, R. A. D.; Vaughan, D. J. Variations in the compositional, textural and electrical properties of natural pyrite: A review. *Int. J. Miner. Process.* **2004**, *74* (1), 41−59.
(28) Appelo, C. A. J.; Postma, D. *Geochemistry, groundwater and pollution*; Balkema, 2007.
(29) Schultz, M. F.; Benjamin, M. M.; Ferguson, J. F. Adsorption and desorption of metals on ferrihydrite: Reversibility of the reaction and sorption properties of the regenerated solid. *Environ. Sci. Technol.* **1987**, *21* (9), 863−869.
(30) Descourvières, C.; Prommer, H.; Oldham, C.; Greskowiak, J.; Hartog, N. Kinetic Reaction Modeling Framework for Identifying and Quantifying Reductant Reactivity in Heterogeneous Aquifer Sediments. *Environ. Sci. Technol.* **2010**, *44* (17), 6698−6705.
(31) Siade, A. J.; Bostick, B. C.; Cirpka, O. A.; Prommer, H. Unraveling biogeochemical complexity through better integration of experiments and modeling. *Environ. Sci.Process. Impacts* **2021**, *23* (12), 1825−1833.
(32) Prommer, H.; Sun, J.; Kocar, B. D. Using reactive transport models to quantify and predict groundwater quality. *Elements (Quebec)* **2019**, *15* (2), 87−92.
(33) Bekele, E.; Page, D.; Vanderzalm, J.; Kaksonen, A.; Gonzalez, D. Water recycling via aquifers for sustainable urban water quality management: Current status, challenges and opportunities. *Water (Switzerland)* **2018**, *10* (4), 457.
(34) Sun, J.; Donn, M. J.; Gerber, P.; Higginson, S.; Siade, A. J.; Schafer, D.; Seibert, S.; Prommer, H. Assessing and Managing Large-Scale Geochemical Impacts From Groundwater Replenishment With Highly Treated Reclaimed Wastewater. *Water Resour. Res.* **2020**, *56* (11), No. e2020WR028066.
(35) Seibert, S.; Prommer, H.; Siade, A.; Harris, B.; Trefry, M.; Martin, M. Heat and mass transport during a groundwater replenishment trial in a highly heterogeneous aquifer. *Water Resour. Res.* **2014**, *50* (12), 9463−9483.
(36) Schafer, D.; Sun, J.; Jamieson, J.; Siade, A. J.; Atteia, O.; Prommer, H. Model-Based Analysis of Reactive Transport Processes Governing Fluoride and Phosphate Release and Attenuation during Managed Aquifer Recharge. *Environ. Sci. Technol.* **2020**, *54* (5), 2800−2811.
(37) Schafer, D.; Sun, J.; Jamieson, J.; Siade, A.; Atteia, O.; Seibert, S.; Higginson, S.; Prommer, H. Fluoride release from carbonate-rich fluorapatite during managed aquifer recharge: Model-based development of mitigation strategies. *Water Res. (Oxf.)* **2021**, *193*, 116880−116880.
(38) NHMRC. Australian drinking water guidelines 6. Version 3.4. National Water Quality Management Strategy.; 2017. https://www.nhmrc.gov.au/sites/default/files/documents/reports/aust-drinking-water-guidelines.pdf (accessed: 2024−March−28).
(39) Corporation Water. Perth Groundwater Replenishment Scheme - Stage 2.; 15837010; Water Corporation: Perth, 2017. http://www.epa.wa.gov.au/sites/default/files/API_documents/GWRS_Stage_2_Referral_Document_Final_-_Revised_Feb_2017_Part1.pdf. (accessed: 2024−March−28).
(40) Norman, J.; Toccalino, P.; Morman, S. *Health-Based Screening Levels for evaluating water-quality data*; US Geological Survey; p 2018.
(41) Harbaugh, A. W. MODFLOW-2005: the U.S. Geological Survey modular ground-water model--the ground-water flow process; 2005. http://pubs.er.usgs.gov/publication/tm6A16 (accessed: 2024−March−28)..
(42) Prommer, H.; Barry, D. A.; Zheng, C. MODFLOW/MT3DMS-based reactive multicomponent transport modeling. *Ground Water* **2003**, *41* (2), 247−257.
(43) White, J. T.; Hunt, R. J.; Fienen, M. N.; Doherty, J. E. Approaches to highly parameterized inversion: PEST++ Version 5, a software suite for parameter estimation, uncertainty analysis, manage-

https://doi.org/10.1021/acs.est.3c10583
Environ. Sci. Technol. 2024, 58, 7567−7576

ment optimization and sensitivity analysis; Reston, VA, 2020. http://pubs.er.usgs.gov/publication/tm7C26 (accessed: 2024−March−28).
(44) Chen, Y.; Oliver, D. S. Levenberg−Marquardt forms of the iterative ensemble smoother for efficient history matching and uncertainty quantification. *Comput. Geosci.* **2013**, *17* (4), 689−703.
(45) White, J. T. A model-independent iterative ensemble smoother for efficient history-matching and uncertainty quantification in very high dimensions. *Environ. Modell. Softw.* **2018**, *109*, 191−201.
(46) Langevin, C. D. Modeling Axisymmetric Flow and Transport. *Groundwater* **2008**, *46* (4), 579−590.
(47) Wallis, I.; Prommer, H.; Post, V.; Vandenbohede, A.; Simmons, C. T. Simulating MODFLOW-Based Reactive Transport Under Radially Symmetric Flow Conditions. *Groundwater* **2013**, *51* (3), 398−413.
(48) Feehley, C. E.; Zheng, C.; Molz, F. J. A dual-domain mass transfer approach for modeling solute transport in heterogeneous aquifers: Application to the Macrodispersion Experiment (MADE) site. *Water Resour. Res.* **2000**, *36* (9), 2501−2515.
(49) Parkhurst, D. L.; Appelo, C. A. J. User's guide to PHREEQC (Version 2): A computer program for speciation, batch-reaction, one-dimensional transport, and inverse geochemical calculations; 1999. https://pubs.usgs.gov/publication/wri994259. (accessed 2024−March−28).
(50) Descourvières, C.; Hartog, N.; Patterson, B. M.; Oldham, C.; Prommer, H. Geochemical controls on sediment reactivity and buffering processes in a heterogeneous aquifer. *Appl. Geochem.* **2010**, *25* (2), 261−275.
(51) Seibert, S.; Atteia, O.; Ursula Salmon, S.; Siade, A.; Douglas, G.; Prommer, H. Identification and quantification of redox and pH buffering processes in a heterogeneous, low carbonate aquifer during managed aquifer recharge. *Water Resour. Res.* **2016**, *52* (5), 4003−4025.
(52) Appelo, C. A. J.; Verweij, E.; Schäfer, H. A hydrogeochemical transport model for an oxidation experiment with pyrite/calcite/exchangers/organic matter containing sand. *Appl. Geochem.* **1998**, *13* (2), 257−268.
(53) Naetscher, L.; Schwertmann, U. Proton buffering in organic horizons of acid forest soils. *Geoderma* **1991**, *48* (1−2), 93−106.
(54) van Breukelen, B. M.; Griffioen, J.; Röling, W. F. M.; van Verseveld, H. W. Reactive transport modelling of biogeochemical processes and carbon isotope geochemistry inside a landfill leachate plume. *J. Contam. Hydrol.* **2004**, *70* (3), 249−269.
(55) Fest, E. P. M. J.; Temminghoff, E. J. M.; Griffioen, J.; Van Riemsdijk, W. H. Proton Buffering and Metal Leaching in Sandy Soils. *Environ. Sci. Technol.* **2005**, *39* (20), 7901−7908.
(56) Sun, N. Z.; Yeh, W. W. G. Coupled inverse problems in groundwater modeling: 2. Identifiability and experimental design. *Water Resour. Res.* **1990**, *26* (10), 2527−2540.
(57) Doherty, J.; Hunt, R. J. Two statistics for evaluating parameter identifiability and error reduction. *J. Hydrol.* **2009**, *366* (1), 119−127.
(58) Doherty, J. E.; Hunt, R. J.; Tonkin, M. J. Approaches to highly parameterized inversion: A guide to using PEST for model-parameter and predictive-uncertainty analysis; Reston, VA, 2010. https://pubs.usgs.gov/publication/sir20105211. (accessed 2024−March−28).
(59) Norton, S. B. Evaluating trace metal mobilization during Managed Aquifer Recharge. *Environmental Engineering Sciences Thesis* Ph.D. thesis; University of Florida: Gainesville, FL, 2011. https://ufdcimages.uflib.ufl.edu/UF/E0/04/35/70/00001/NORTON_S.pdf. (accessed 2024−March−28).
(60) Dzombak, D. A.; Morel, F. M. *Surface complexation modeling: Hydrous ferric oxide*; John Wiley & Sons, 1990.
(61) Stumm, W.; Sigg, L.; Sulzberger, B. *Chemistry of the solid-water interface: processes at the mineral-water and particle-water interface in natural systems*; Wiley, 1992.
(62) Nordstrom, D. K.; Blowes, D. W.; Ptacek, C. J. Hydrogeochemistry and microbiology of mine drainage: An update. *Appl. Geochem.* **2015**, *57*, 3−16.
(63) Nordstrom, D. K. Hydrogeochemical processes governing the origin, transport and fate of major and trace elements from mine wastes and mineralized rock to surface waters. *Appl. Geochem.* **2011**, *26* (11), 1777−1791.
(64) Blowes, D. W.; Ptacek, C. J.; Jambor, J. L.; Weisener, C. G.; Paktunc, D.; Gould, W. D.; Johnson, D. B. 11.5 - The Geochemistry of Acid Mine Drainage. In *Treatise on Geochemistry*; 2nd ed., Holland, H. D.; Turekian, K. K. Eds.; Elsevier, 2014; pp. 131190.
(65) Fischler, C.; Hansard, P.; Ladle, M.; Burdette, C. A Review of Selected Florida Aquifer Storage and Recovery (ASR) Sites and Their Geochemical Characteristics; Florida Geological Survey, 2015. https://ufdcimages.uflib.ufl.edu/AA/00/03/84/34/00001/RI-112.pdf (accessed 2024−March−28).

https://doi.org/10.1021/acs.est.3c10583
Environ. Sci. Technol. 2024, 58, 7567−7576